P1.4 ON THE DIURNAL CYCLE IN A STRATOCUMULUS-TOPPED MIXED LAYER

Yunyan Zhang *, Bjorn Stevens, Michael Ghil
University of California at Los Angeles, Los Angeles, California

1. Introduction

The mixed-layer model (MLM) introduced by Lilly (1968) provides the theoretical framework upon which most of our understanding of the marine stratocumulus-topped boundary layer (STBL) is based. Even so, this model has been called into question by the perception that it is unable to adequately represent several major aspects of the STBL diurnal cycle. Schubert (1976) (hereafter S76) showed that the cloud base descends at a rate somewhat greater than that of the cloud top, which leads to cloud thickening during the daytime. However, observations have shown the diurnal evolution of marine stratocumulus to be characterized by an ascending (Vernon, 1936; Hignett, 1991) or a relatively constant cloud base (Bretherton et al., 2003), but not a descending one. This discrepancy has fueled the idea that decoupling between the cloud layer and the surface plays an essential role in the dynamics of the STBL (Turton and Nicholls, 1987). This idea, too, seems inconsistent with the data during East Pacific Investigation of Climate (EPIC, Bretherton et al., 2003) – wherein the observed boundary layers appeared to remain relatively well mixed throughout the diurnal cycle. Schubert's parameterization of entrainment was formulated in a way which precludes the study of the relatively weak entrainment efficiencies that appear to be more representative of actual clouds (Lewellen and Lewellen, 1998; vanZanten et al., 1999; Stevens, 2002). The puzzling behavior of the MLM diurnal cycle might thus be an artifact of the entrainment parameterization employed. We shall see that the diurnal cycle does show marked sensitivity to entrainment efficiency.

2. Mixed-layer model and entrainment closure

The MLM we use is Stevens' (2002) version of Lilly's (1968) model. The STBL is assumed to be well-mixed throughout its depth and possess horizontally homogeneous thermodynamic fields. Mixing is mainly driven by radiative cooling at the cloud top. For a given surface pressure, the state of this bulk layer is uniquely determined by its depth h (also the height of mixed layer and cloud top), liquid-water static energy $s_l = c_p T + gz - L_v q_l$ and total-water specific humidity $q_t = q_v + q_l$, where c_p is the specific heat capacity, T the air temperature, g the gravity, z the height above the surface, L_v the latent heat of vaporization, q_l the liquid-water specific humidity and q_v the water-vapor specific humidity. s_l and q_t are approximately invariant following isoentropes in the moist systems.

The prognostic equations for h, s_l and q_t are:

$$\frac{dh}{dt} = E - Dh \tag{1}$$

$$h\frac{d}{dt}\langle s_l\rangle = V(s_{l,0} - \langle s_l\rangle) + E(s_{l,+} - \langle s_l\rangle) - \frac{\triangle F_s}{\rho} \tag{2}$$

$$h\frac{d}{dt}\langle q_t\rangle = V(q_{t,0} - \langle q_t\rangle) + E(q_{t,+} - \langle q_t\rangle) - \frac{\triangle F_q}{\rho} \tag{3}$$

In the above,

$$\langle \mathcal{X}\rangle = \frac{1}{h}\int_0^h \mathcal{X} dz \tag{4}$$

stands for the vertical averaged, or bulk value, and $\mathcal{X} \in (s_l, q_t)$. Subscript 0 and + denote surface values and the states just above cloud top respectively, while $\triangle F_s$ and $\triangle F_q$ are the diabatic forcings. Specifically, $\triangle F_s$ consists of the radiative driving, $\triangle F_R$, and the drizzle effect on liquid-water content in s_l, while $\triangle F_q$ is the drizzle effect on q_t. ρ is the air mass density and D represents the large-scale divergence. Surface fluxes are calculated by a bulk aerodynamic formula, where $V = C_D\|U\|$, with $\|U\|$ the surface wind speed, and C_D the surface exchange coefficient, which is assumed constant. Equation (1) essentially defines E, the entrainment rate, as the diabatic growth rate of the mixed-layer depth.

An entrainment parameterization is needed to close the system (1) – (3). In this study, two entrainment parameterizations are investigated: one following S76, and the other following Lewellen and Lewellen (1998) (hereafter LL98). S76 obtains a value for E by constructing the buoyancy flux profile as:

$$\mathcal{B}_{min} = -\frac{2k}{1-k}\langle \mathcal{B}\rangle \tag{5}$$

where usually $k = 0.2$, $\mathcal{B}_{min}$ is the vertical minimum of the buoyancy flux, and $\langle \mathcal{B}\rangle$ is the bulk value of $\mathcal{B}$ defined in (4) in above. In LL98 parameterization, the single control parameter is the entrainment efficiency defined as follows:

$$\eta = \frac{\int_0^h (\mathcal{B}_{NE} - \mathcal{B})dz}{\int_0^h \mathcal{B}_{NE} dz} \tag{6}$$

* *Corresponding author address:* Yunyan Zhang, Dept. of Atmospheric and Oceanic Sciences, University of California at Los Angeles, 405 Hilgard Ave., Box 951565, Los Angeles, CA 90095-1565; e-mail: yunyan@atmos.ucla.edu

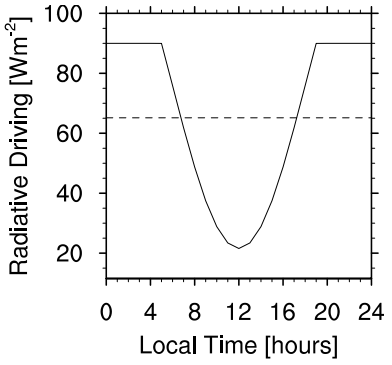

Figure 1: Diurnal variation of $\triangle F_R$, the radiative driving at cloud top. Dashed line illustrates the daily average.

where $\mathcal{B}$ is the buoyancy flux, and $\mathcal{B}_{NE}$ is its value if there is no entrainment.

The advantage of LL98 is that varying η between 0 and 1 samples the full range of entrainment efficiencies. This is in contrast to the S76 closure, wherein the variation of the entrainment parameter k in (5) between 0 and 1 samples only a range of entrainment efficiencies that corresponds roughly to $0.6 < \eta < 1.0$.

The model results produced by the S76 entrainment rule (5) with $k = 0.2$ are quite similar to the LL98 results with $\eta = 0.77$. To simplify the analysis we take advantage of this result and use LL98 with $\eta = 0.77$ to substitute for S76 with $k = 0.2$ in the following study; our arguments can thus be expressed entirely in terms of entrainment efficiencies. Although not shown, we have checked that any conclusion drawn based on LL98 with $\eta = 0.77$ does indeed hold for the S76 rule with $k = 0.2$.

The liquid-water path L is:

$$L = \int_b^h \rho q_l dz \tag{7}$$

where b denotes the cloud base height that can be diagnosed from s_l and q_t. L is proportional to $(h - b)^2$. Hereafter our discussion will be focused on L instead of simply cloud thickness.

3. STBL diurnal variation

For the diurnal cycle modeling, following S76, we assume the STBL is non-precipitating and evolves through a succession of quasi-steady states, as described by Stevens (2002). Therefore in (2) and (3), $\triangle F_q = 0$ and $\triangle F_s$ equals simply $\triangle F_R$, the radiative driving. Infrared (IR, also referred to as long wave) cooling and solar (also referred to as short wave) heating both occur in fact through certain finite depths in the cloud layer, but we assume here that the net radiative driving is located only at cloud top, this being consistent with the boundary projection method used by Stevens (2002).

The cyclic pattern of the radiative driving is chosen, for reasons of consistency, to follow S76, with sunrise at 0500 LST and sunset 1900 LST (see Figure 1). Due to the combined effect of IR cooling and solar heating, $\triangle F_R$ decreases from dawn to noon, reaching a minimum of 20 Wm^{-2}. It then increases from noon till dusk. At night only outgoing IR cooling is present, so $\triangle F_R$ stays constant at 90 Wm^{-2}. Prescribed large-scale conditions are listed in Table 1.

Table 1: Boundary Conditions

Large-scale divergence (D)	$6 * 10^{-6}$ s^{-1}
Surface wind speed ($\|U\|$)	7 ms^{-1}
Sea surface temperature (SST)	290 K
Specific humidity above cloud ($q_{t,+}$)	3.5 g/kg

Table 2: Initial Conditions

Variable	$\eta = 0.77$	$\eta = 0.20$
h	1002.5 m	717.5 m
$\theta_l \approx s_l/c_p$	291 K	288 K
q_t	8.2 g/kg	8.9 g/kg

To illustrate the sensitivity of the simulated STBL diurnal cycle to the entrainment efficiency, we investigate two cases: one with $\eta = 0.20$ and the other with $\eta = 0.77$. Initial conditions are listed in Table 2. Each experiment is started from its equilibrium corresponding to $\triangle F_R =$ 65 Wm^{-2}, the daily average of $\triangle F_R$.

Figure 2 illustrates the diurnal cycle for the model using the LL98 closure with $\eta = 0.77$, while the case with $\eta = 0.20$ is shown in Figure 3. The transient solutions (heavy curves in both figures) show the results for the full time-dependent calculation using (1)–(3) with diurnally varying radiative driving, while the equilibrium solutions (light curves) indicate equilibrium calculations in which MLM variables adjust to the instantaneous value of the radiative driving, assumed to be constant, at each time of day. The shallower boundary layer and thicker cloud in Figure 3 reflect the effectively weaker entrainment for $\eta = 0.20$ (cf. Stevens, 2000).

In both figures the transient cloud top height h achieves its maximum around 0600 LST and its minimum around 1700 LST. With $\eta = 0.77$, however h is larger and also has a larger diurnal variation than for the case with $\eta = 0.20$. In Figure 2 the transient cloud base height b exhibits a marked diurnal variation with an amplitude of about 90 meters. In contrast, in Figure 3 the transient b remains relatively constant, which is more consistent with the EPIC data (Bretherton *et al.*, 2003). With $\eta = 0.77$, the transient L increases during the day. By $\eta = 0.20$, L is nearly out of phase with the previous result.

According to our simulations, such differences are found not only between these two specific cases, but across the full range of entrainment efficiencies. Clearly entrainment efficiency has a pronounced effect on the STBL's diurnal evolution. What causes these differences? The equilibrium solutions for h, b, and L, also plotted in Figures 2 and 3, help us address this question. The equilibrium solutions for L are very similar in the two cases of $\eta = 0.77$ and $\eta = 0.20$: both

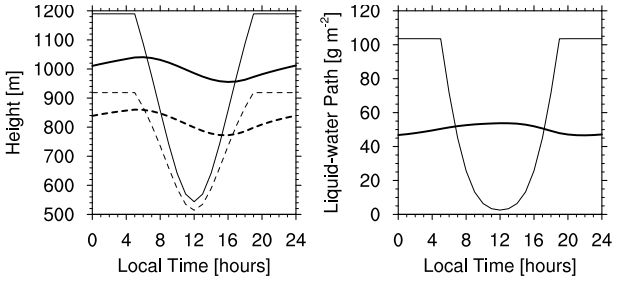

Figure 2: MLM results for the STBL diurnal variation when using the LL98 entrainment rule with $\eta = 0.77$. In the left panel, transient mixed-layer depth (heavy solid line) and its equilibrium solution (light solid line); transient cloud base (heavy dashed line) and its equilibrium solution (light dashed line). In the right panel, transient liquid-water path (heavy solid line) and its equilibrium solution (light solid line). This is a good approximation for the behavior using S76 closure with $k = 0.2$.

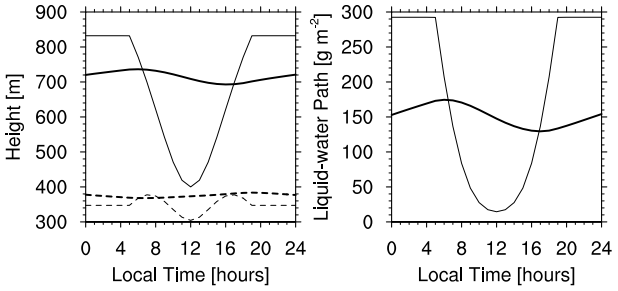

Figure 3: As in Figure 2, but with $\eta = 0.20$.

show a pronounced minimum when radiative driving has a minimum. This implies that if the MLM were always in instantaneous equilibrium with its forcing, the diurnal cycle of L would be relatively insensitive to the entrainment closure. Consequently, the differences in the transient behavior, in which the phase of the STBL diurnal cycle shifts with entrainment efficiency, must result from differences in the adjustment processes.

To explore this idea, it is useful to introduce a simplified system of equations, in which the transient variations follow the changes in the equilibrium state of the STBL:

$$\frac{d\chi}{dt} = -\frac{\chi - \chi_e(t)}{\tau_\chi} \tag{8}$$

where $\chi \in (h, \langle s_l \rangle, \langle q_t \rangle)$ and subscript e stands for the equilibrium solution. Note that χ_e are functions of time and evolve with $\triangle F_R$, while τ_h, τ_s and τ_q are the adjustment timescales for h, $\langle s_l \rangle$ and $\langle q_t \rangle$ respectively. As shown by Schubert et al. (1979), the magnitude of τ_h is approximately one week, which is determined by large-scale subsidence; while one day for τ_s and τ_q, determined by the STBL thermodynamics. Note that τ_h is generally much larger than τ_s and τ_q.

In the mixed-layer framework, L essentially represents $(h - b)$. What controls the transient h? As shown in Figures 2 and 3, at night, the STBL is in a constant equilibrium state, which corresponds to the fixed IR cooling of 90 Wm^{-2} (see Figure 1). After dawn, solar heating abates IR cooling and h_e changes rapidly with time. Note that, in Figures 2 and 3, the sign of dh/dt is indeed given by the sign of $(h_e - h)$, as would be expected if $h(t)$ were actually governed by (8). This adjustment causes h to lag h_e by several hours. What controls the transient b? In our MLM, the cloud base height is diagnosed from the total specific humidity and the air temperature, which can be derived from the liquid-water static energy. Therefore b adjusts to its equilibrium value b_e, with a timescale that is determined by that of the thermodynamic quantities, τ_s and τ_q. In Figure 2, the diurnal cycle of b_e is very similar to that of h_e. Although $(h - h_e) > (b - b_e)$, the adjustment timescale τ_h is much longer than τ_s and τ_q: consequently the cloud base descends more rapidly than the cloud top causing the layer to thicken as it adjusts to the changing forcing. In contrast b_e shows a week diurnal variation in Figure 3. In this case, $(b - b_e)$ is so small that $db/dt < dh/dt$. Thus the transient b is very nearly constant, and hence the variation in h dominates the diurnal evolution of L.

Two distinct processes are evident in the STBL behavior discussed above. First, h and b adjust to their equilibria on different timescales. Second, b_e varies significantly with the entrainment parameterizations being used. The equilibrium solutions and the adjustment timescales together determine the evolution of L.

To understand more clearly the STBL behavior in Figures 2 and 3, it is useful to ask how η influences b_e. To make the problem analytically tractable, we define a radiative entrainment efficiency α:

$$\alpha = \frac{E \triangle s_l}{\triangle F_R} \tag{9}$$

where $\triangle s_l = s_{l,+} - \langle s_l \rangle$. The value of α depends, of course, on the entrainment rule and it is not constant in general. By investigating solutions at constant α, we can, however, develop insights into how η affects the equilibrium state.

Given (9), h_e, $\langle s_l \rangle_e$ and $\langle q_t \rangle_e$ can be written as:

$$h_e = h_0 \left(\frac{\alpha}{1 + \sigma - \alpha}\right) \tag{10}$$

$$\langle s_l \rangle_e = s_{l,0} - (s_{l,+} - s_{l,0}) \left(\frac{1 - \alpha}{\sigma}\right) \tag{11}$$

$$\langle q_t \rangle_e = q_{t,0} + (q_{t,+} - q_{t,0}) \left(\frac{\alpha}{1 + \sigma}\right) \tag{12}$$

where

$$\sigma = \frac{V(s_{l,+} - s_{l,0})}{\triangle F_R} \qquad \text{and} \qquad h_0 = \frac{V}{D}$$

$(s_{l,+} - s_{l,0})$ represents the lower troposphere stability, which is relatively constant and positive, while the value of $(q_{t,+} - q_{t,0})$ is usually negative.

If α remains constant, σ captures the diurnal cycle of $\triangle F_R$ in the equilibrium solutions. At night, only IR cooling is present so σ is fixed, and the equilibrium solutions remain constant. In the morning $\triangle F_R$ begins to decrease and thus σ increases, leading to an increase in

$\langle s_l \rangle_e$ and $\langle q_t \rangle_e$, and a decrease in h_e. Cloud base rises as the STBL warms and dries. An increase in both $\langle s_l \rangle_e$ and $\langle q_t \rangle_e$ have counteracting influences on cloud base height. In the afternoon, solar heating begins to decrease and the evolution is reversed.

For different entrainment efficiencies, however, the diurnal evolution and effect of α differs. In general, α is larger for higher entrainment efficiencies. A diurnal evolution in α is to be expected, given the differing degree to which $\triangle F_R$ contributes to the TKE production throughout the course of the diurnal cycle, but we neglect this evolution for the moment. From (11)–(12), the amplitude of the diurnal cycle in b_e depends on α. We consider two limits: $\alpha = 1$ for high entrainment efficiency while $alpha = 0$ for low entrainment efficiency. As α becomes large, the diurnal cycle of $\langle s_l \rangle_e$ will be diminished, while that of $\langle q_t \rangle_e$ is enhanced. When $\alpha = 1$, $\langle s_l \rangle_e$ will remain constant throughout the day, while the diurnal cycle in $\langle q_t \rangle_e$ dominates other diurnal variations; this will result in a lowering of b_e. As α approaches 0, the diurnal cycle of $\langle q_t \rangle_e$ disappears, while the diurnal effect of $\langle s_l \rangle_e$ is amplified; this will result in a rising of b_e. This discussion suggests that α mediates between the competing effects of $\langle s_l \rangle_e$, and $\langle q_t \rangle_e$ on b_e. Overestimating entrainment produce a significant increase in the diurnal variation of the cloud base, especially in its lowering.

4. SUMMARY

We examined the diurnal cycle of the stratocumulus-topped boundary layer (STBL). Our study emphasized the sensitivity of the mixed-layer representation of the STBL to the model's entrainment efficiency η.

The marked sensitivity of the diurnal cycle to η is found to depend on both the equilibrium heights of cloud boundaries for a fixed diurnally varying radiative driving and the timescales at which these heights adjust to their equilibria. The adjustment timescale for cloud top is determined by the dynamic factor, *i.e.*, the large-scale subsidence; the timescale for cloud base is determined mainly by the STBL thermodynamics, *i.e.*, the water and heat budgets. It turns out the former timescale is much greater than the latter.

In the case of high entrainment efficiencies, a pronounced diurnal variation is found in the instantaneous equilibria of both cloud boundaries. This behavior results in comparable distances between the results for cloud boundary height from a time-dependent MLM calculation and its equilibrium value for both boundaries. Because of the distinct adjustment timescales, however, the descent rate of the cloud top is less than the one of the cloud base, which leads to cloud thickness growing during the daytime. In the case of low entrainment efficiencies, a pronounced diurnal variation is found in the equilibrium height of cloud top but not in cloud base. Hence the descending behavior of the cloud top governs the daytime evolution of cloud thickness, irrespective of the adjustment timescales.

Having defined a radiative entrainment efficiency rate α, we further explored how different entrainment efficiencies may influence the equilibria of the STBL.

In summary, a better diurnal variation of cloud thickness can be produced by mixed-layer theory when using low entrainment efficiencies. The success of an MLM under these circumstances suggests that diurnal decoupling between the cloud layer and the surface may be less important than previously thought.

References

Bretherton, C. S., T. Uttal, C. W. Fairall, S. E. Yuter, R. A. Weller, D. Baumgardner, K. Comstock, and R. Wood, 2003: The EPIC 2001 stratocumulus study. *Bull. Amer. Meteor. Soc.*, accepted.

Hignett, P., 1991: Observations of diurnal variation in a cloud-cappedmarine boundary layer. *J. Atmos. Sci.*, **48**, 1474–1482.

Lewellen, D., and W. Lewellen, 1998: Large-eddy boundary layer entrainment. *J. Atmos. Sci.*, **55**, 2645–2665.

Lilly, D. K., 1968: Models of cloud topped mixed layers under a strong inversion. *Quart. J. R. Met. Soc.*, **94**, 292–309.

Schubert, W. H., 1976: Experiments with lilly's cloud-topped mixed layer model. *J. Atmos. Sci.*, **33**, 436–446.

Schubert, W. H., J. S. Wakefield, E. J. Steiner, and S. K. Cox, 1979: Marine stratocumulus convection. Part II: horizontal inhomogeneous solutions. *J. Atmos. Sci.*, **36**, 1308–1324.

Stevens, B., 2000: Cloud transitions and decoupling in shear-free stratocumulus-topped boundary layers. *Geophys. Res. Lett.*, **27**, 2557–2560.

Stevens, B., 2002: Entrainment in stratocumulus-topped mixed layers. *Quart. J. R. Met. Soc.*, **128**, 2663–2690.

Turton, J. D., and S. Nicholls, 1987: A study of the diurnal variation of stratocumulus using a multiple mixed layer model. *Quart. J. R. Met. Soc.*, **113**, 969–1009.

vanZanten, M. C., P. G. Duynkerke, and J. W. M. Cuijpers, 1999: Entrainment parameterization in convective boundary layers. *J. Atmos. Sci.*, **56**, 813–828.

Vernon, E. M., 1936: The diurnal variation in ceiling height beneath stratus clouds. *Mon. Wea. Rev.*, **64**, 14–16.